ELSEVIER

Journal of Alloys and Compounds 320 (2001) 326–340

Journal of ALLOYS AND COMPOUNDS

www.elsevier.com/locate/jallcom

Systematics of lanthanide and actinide compound formation: remarks on the americium alloying behaviour

R. Ferro*, G. Cacciamani, A. Saccone, G. Borzone

Dipartimento di Chimica e Chimica Industriale, Università di Genova, Via Dodecaneso 31, 16146 Genova, Italy

Abstract

General characteristics of binary lanthanide and actinide alloys are briefly reviewed and compared. Compound formation capability and thermodynamics (both experimental and estimated data) are especially considered and discussed. These data are then used to assess and predict the americium alloying behaviour. A systematic short description is finally given of the available, and estimated, data relevant to the different Am–Me systems with the various Me elements. © 2001 Elsevier Science B.V. All rights reserved.

Keywords: Americium alloys; Americium compounds; Alloy thermodynamics; Actinides; Lanthanides

1. Introduction

It is well known that systematics may have a relevant role in the description and classification of the alloying behaviour of a specific element or group of elements, especially regarding certain characteristics. Typically the influence on the properties of the alloys of elemental 'factors', such as atomic dimensions, electron valence concentration, etc. have often been studied and some prediction procedures discussed [1–3].

A well known example of a simple application may be given by the classification of the different elements according to their influence, in the Fe alloys, on the Fe transformation temperatures, the extension of the α or γ solubility fields, etc. [4].

Another example may be represented by the categorisation of the elements into four groups according to the types of binary phase diagrams they give with Ti, specifically according to the relative stabilisation of the α and β Ti solid solutions and the features of the related transformation equilibria [5].

Wider applications of the systematics may be found in the description and classification of the alloying behaviour of selected groups of elements (such as alkaline earth metals, lanthanides, actinides, etc.) which, having similar properties, may be jointly discussed.

The availability of criteria for a systematic, albeit empirical, classification of the different alloys has an obvious interest also for checking specific experimental results, interpolating and/or predicting data, equilibria, etc.

In a very general way this problem has been faced by Villars et al. [6]: they used pattern recognition (learning machines) techniques to elaborate large data sets and find parameters useful for a systematic description and prediction of properties (such as compound formation in metallic systems, their crystal structures, etc.).

We are mainly interested in the alloying behaviour of the lanthanides (Ln) and actinides (An). For these elements, and particularly for the Ln, the systematics has been frequently and successfully used for predicting or interpolating properties. The Ln, in fact, mainly the trivalent ones, show regular smooth trends, as a function of the atomic number, in several constitutional properties of the pure elements and of their alloys (see Figs. 1–5).

For the actinides more complex trends have been observed, as exemplified in the same Figs. 1–5. Owing to their position in the Periodic Table, analogies and differences with the Ln have been pointed out several times, by studying both elemental properties and compound characteristics. This may be shown by Fig. 6, where different schemes of comparison between the Ln and An behaviours are presented.

From this figure it is apparent that it is not possible to find a simple relation between the properties of the elements having the same position in the two rows. This may be related also to the remarks made by Smith and Kmetko [7] and summarised in Fig. 7. In this figure the transition metals are arranged in order of decreasing

---

*Corresponding author. Tel.: +39-010-353-6149; fax: +39-010-362-5051.

E-mail address: ferro@chimica.unige.it (R. Ferro).

0925-8388/01/$ – see front matter
PII: S0925-8388(00)01470-5

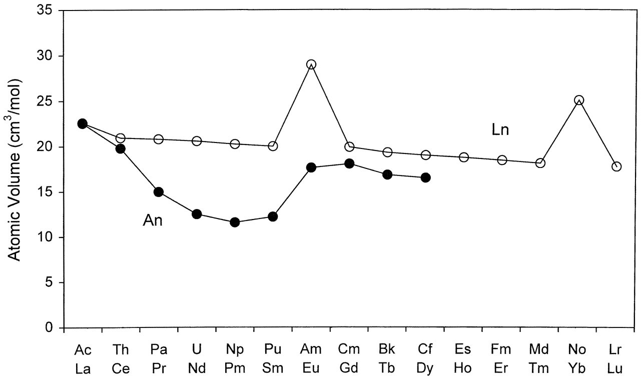

Fig. 1. Compared trends of the Ln (○) and An (●) atomic volumes in the crystalline state stable at room temperature.

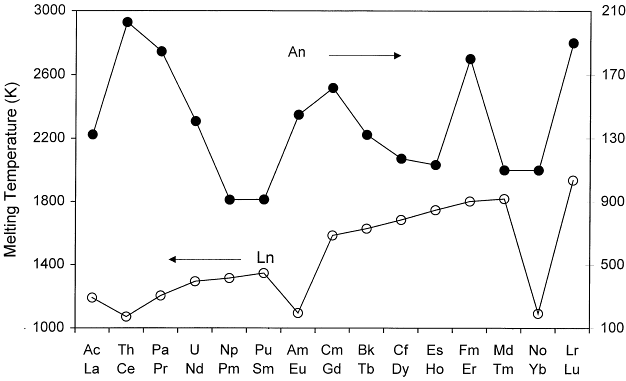

Fig. 2. Compared trends of the Ln (○) and An (●) melting temperatures.

localisation of the d or f electrons. The diagonal strip (shaded elements) is the boundary region: crossing this region from left to right can be viewed as a Mott transition from a metallic to an insulating magnetic state for the relevant d or f electrons. According to Ref. [7] materials close to this delocalisation–localisation transition can have their properties modified appreciably by small perturbations. For example the pure elements on the diagonal strip possess a large number of allotropic crystal structures which can be alternately stabilised by temperature and/or pressure variations. As an example it may be very useful to make a comparison between the series of elemental structures shown by Ln [1] and An [8] and their dependence on P and T.

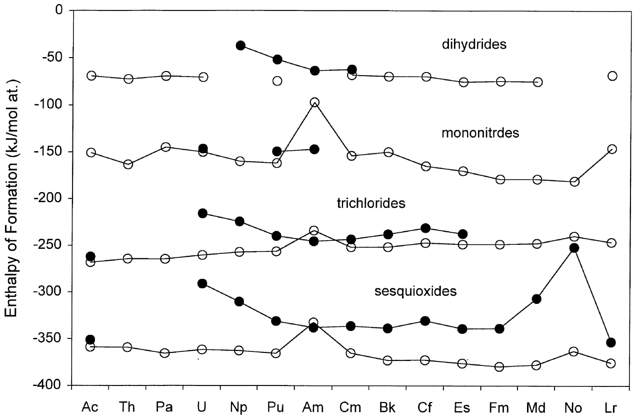

Fig. 3. Compared trends of the enthalpies of formation of selected Ln (○) and An (●) non-metallic compounds (for the heavier An, estimated values have been used).

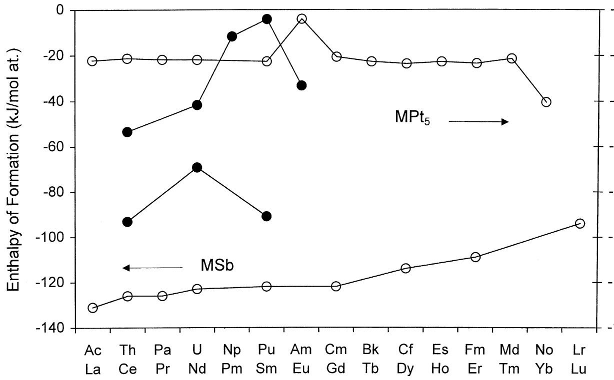

Fig. 4. Compared trends of the experimental enthalpies of formation of selected Ln (○) and An (●) intermetallic compounds.

A kind of summary of the similarities, albeit with some uncertainties, which may be evidenced between the single Ln and An is reported in Fig. 8; in particular it may be observed that, according to this scheme, a clear set of similarities relates the block of elements from Pr to Sm, on one side, with the elements from Am to Cf.

These trends and similarities may be useful for checking and predicting data mainly for elements for which the experimental investigation is especially difficult (Pm or the heavy An, for instance).

The transplutonium metals in particular represent a group of elements for which it may be considered particularly useful the assessment of a set of reliable criteria for a classification and categorisation of the still largely incomplete data about alloy and compound formation. As observed by Gibson et al. [9] the field of phase relations in alloy systems comprising actinides has recently received renewed attention, as a result, for instance, of proposed new waste-remediation technologies which may incorpo-

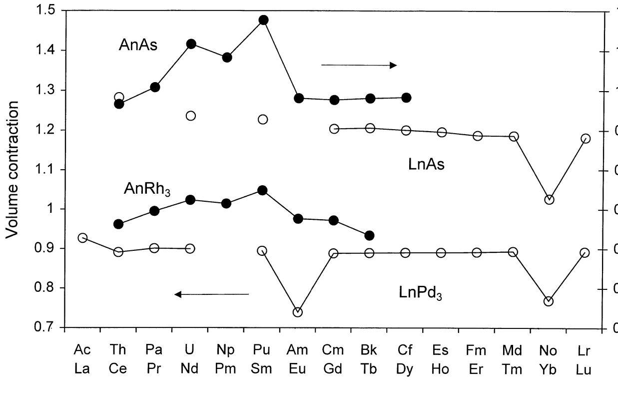

Fig. 5. Compared trends of the volume contractions of selected Ln (○) and An (●) intermetallic compounds.

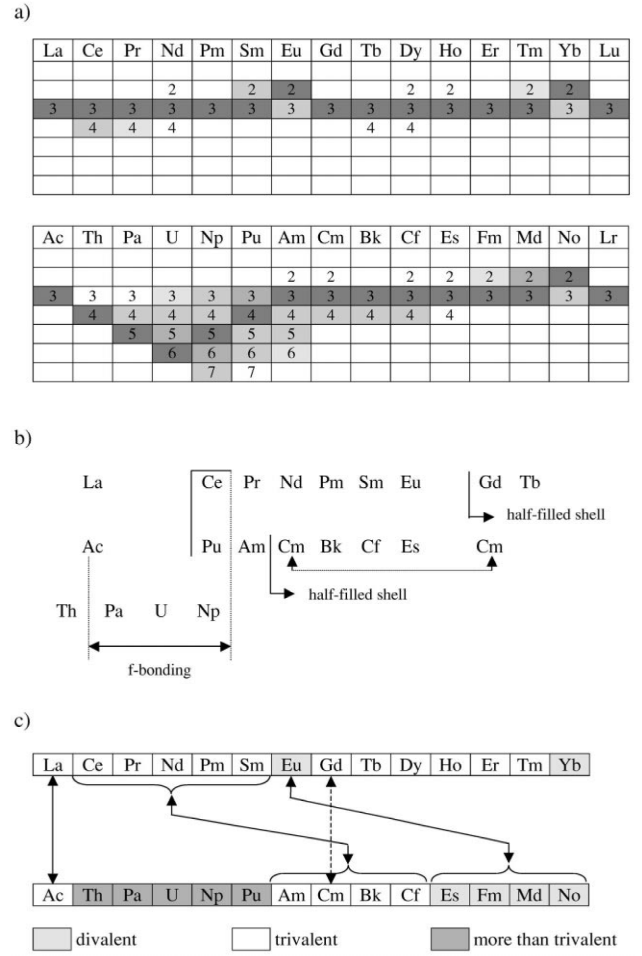

a)

La	Ce	Pr	Nd	Pm	Sm	Eu	Gd	Tb	Dy	Ho	Er	Tm	Yb	Lu
			2		2	2			2	2		2	2	
3	3	3	3	3	3	3	3	3	3	3	3	3	3	3
	4	4	4					4	4					

Ac	Th	Pa	U	Np	Pu	Am	Cm	Bk	Cf	Es	Fm	Md	No	Lr
						2	2		2	2	2	2	2	
3	3	3	3	3	3	3	3	3	3	3	3	3	3	3
	4	4	4	4	4	4	4	4	4	4				
		5	5	5	5	5								
			6	6	6	6								
				7	7									

Fig. 6. Schemes of comparison and likeness between Ln and An behaviour in typical chemical states: (a) oxidation states in general; (b) analogies between Ln and An on the basis of the hydride properties [22]; (c) analogies between Ln and An and their valence in metallic state.

rate actinides into metallic matrices. Emphasis has also been given to the interest that the properties of these actinides materials may have from a fundamental perspective.

Among these metals americium may be especially important and interesting in view of recently suggested applications. According to Rubbia [10], ^{242}Am may represent the fuel for a new fission fragment heated propulsion system applicable to manned missions to the planet Mars.

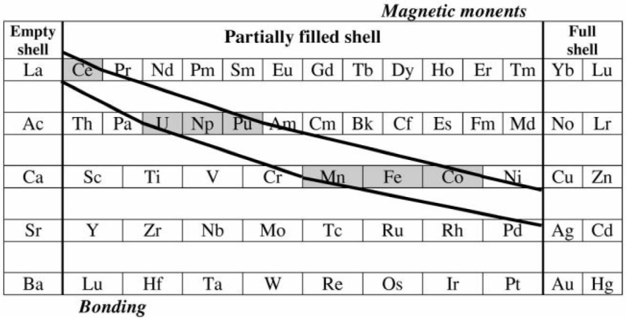

Fig. 7. Table of the d and f transition elements showing the cross-over between electron bonding and magnetic moment formation, according to Ref. [7].

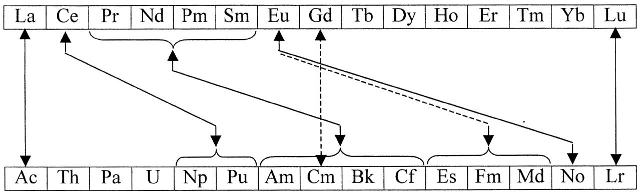

Fig. 8. Table of correspondence between Ln and An elements assumed in this work on the basis of the similarities suggested by several authors.

Chemical problems due to the reactivity of Am, for instance with H_2 (the propellant), C and BeO (possible supporting materials for Am deposited as a layer), etc. will be important.

Their description could be fruitfully approached in the framework of systematics; this paper will specially concern this point.

2. Remarks on lanthanide and actinide compound formation

A first point to be considered refers to the compound formation in the different Ln–X and An–X systems. A scheme of this behaviour is reported in Fig. 9.

As a first approximation we notice a similar behaviour for the lanthanides (both light and heavy trivalent Ln, represented by La and Gd, respectively, and divalent Eu and Yb) and the actinides (for these Th, U, Np and Pu have been selected on the basis of the information available).

Generally we notice formation of compounds with the elements on the right of the Periodic Table, typically from the seventh group on. The elements on the left (with some exceptions for the lightest ones, Be, Mg, etc.) do not form any intermediate phases; their binary phase diagrams with Ln or An are generally of the simple eutectic or monotectic type. For some of the actinides, however, the formation by solid-state reaction of some phases stable only at low temperature has also been observed.

Considering the general validity of this subdivision, it may be assumed that it is also applicable to the heavy transplutonium actinides. For Am, the data reported in Fig. 10, which represent the only available information on its compound formation capability, even though approximate and incomplete, is in agreement with the mentioned general behaviour.

A more detailed examination of the compounds formed by the different elements with the Ln and An show a change in their stability on passing from one position to another in the Periodic Table. Generally we have two regions of high stability: one around the ‘noble metals’ and the other for the more electronegative elements with a a)

La

1															
	1											3	2	1	1
	6											6	5	4	2
	0	0	0	0	0	0	0	8	8	5	8	5	6	3	5
		0	0	0	0		5	8	5	4	5	7	9	5	4
	0	Ln		0	0	0	2	10	6	5	6	6	7	5	
		An													

Eu

1															
	1											1	4	1	3
	5											3	2	8	3
	0	0	0	0	0	0	1		3	4	5	6	5	12	1
		0	0	0	0	0		4	7	5	7	4	2	4	3
	0	Ln	0	0	0	1		2	7	7	4	3	4	5	1
		An													

Gd

2															
	1											5	4	1	1
	4											5	5	2	4
	0	0	0	0	0	3	4	8	9	7	10	5	7	1	2
		0	0	0	0	1	4	9	8	3	6	5	10	4	6
	0	Ln		0	0	1	2	7	8	8	4	6	6	4	
		An													

Yb

2															
	1											5	6	1	2
	1											2	4	2	6
	0		0	0	0	0	2	3	5	5	8	7	2	3	3
		0	0	0	0		2	3	9	6	6	5	5	6	3
	0	Ln	0	0	0	1	1	4	9	8	5	4	5	5	1
		An													

b)

Th

2															
	1											3	2	3	1?
1	2											7	4	4	5
		0	0	0	0	3	5	5	7	4	4	4	6	3	5
		0	0	0	0		4	7	7	3	6	4	4	3	4
	0	Ln	0	0	0	3	3	6	8	6	4	5	4	6	
		An													

U

1															
0	1											3	3	5?	6?
0	0											3	7	2+	6
	0	0	[1]	0	0	2	2	6	7	1	2	3	7	3	7
		0	[1]	0	[1]		5	4	5	0	1?	5	5	4	10
		Ln	0	0	0	2	4	5	4	2	4	1+	2	3	
		An													

Np

	1											5	3	1	4
												3	2	2	3
					0?	2+	1	1+	1+			2		3	4
			[1]				1	1	1		2		2	2	4
		Ln				1	1	1	3		2?	1		1	
		An													

Pu

0															
0	1											5	4	1	4
0	3											5	5	1+	3+
0	0	[1]	0	0	0	1	2	6	6	4	6	12	6	1+	4+
	0	0	[1]	0	0		5	8	4	2	4	5	7	2+	2+
	0	Ln	[2]	0	0	1	4	4+	8	8	2	2+	6	3	
		An													

Fig. 9. Indicative number of compounds formed in the binary Ln–X (a) and An–X (b) systems. For each element of the groups 1–16, represented by its position in the Periodic Table, the number of compounds observed in the binary systems with selected Ln or An is reported. Symbols used: *n*, number of known compounds; *n*+, more compounds, not yet observed, are probably present; [*n*], compounds are stable only at relatively low temperature and decompose before melting; 0, it is known that no compounds are formed; ?, the compound formation is uncertain; blank, no information.

gradual stability increase moving to the far right of the Periodic Table.

This may be summarised by the data available for the thermodynamics of these systems and specifically by the data available on the enthalpy of formation. The experimental values of the $\Delta_f H$ of the binary compounds of a generic Ln (values averaged from different Ln are reported) and of U are given, as an example, in Fig. 11. We notice a subdivision of the table, according to the sign of $\Delta_f H$, which is in agreement with the data shown in Fig. 9.

In the same figure the experimental values are compared with those computed according to the Miedema model: a good agreement is generally observed between the experimental and computed schemes. A few exceptions may be noticed: see for instance carbon, for which large discrepancies between calculated and experimental values are observed for both Ln and An.

Especially interesting may be the indication given by the correlation between the Miedema enthalpy value and the compound formation capability. As pointed out in Ref. [2], a relation may be deduced between the average number of stable intermediate phases in a binary system and the

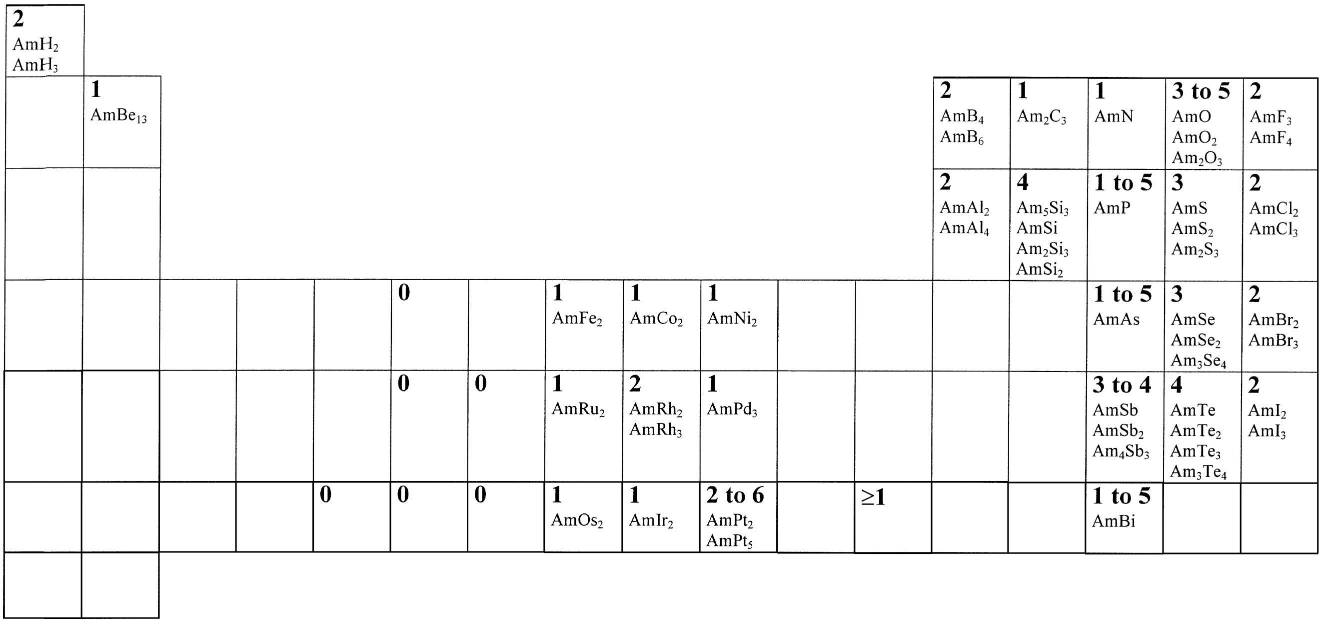

2 AmH_2 AmH_3																
	1 $AmBe_{13}$											**2** AmB_4 AmB_6	**1** Am_2C_3	**1** AmN	**3 to 5** AmO AmO_2 Am_2O_3	**2** AmF_3 AmF_4
												2 $AmAl_2$ $AmAl_4$	**4** Am_5Si_3 AmSi Am_2Si_3 $AmSi_2$	**1 to 5** AmP	**3** AmS AmS_2 Am_2S_3	**2** $AmCl_2$ $AmCl_3$
					0		**1** $AmFe_2$	**1** $AmCo_2$	**1** $AmNi_2$					**1 to 5** AmAs	**3** AmSe $AmSe_2$ Am_3Se_4	**2** $AmBr_2$ $AmBr_3$
					0	**0**	**1** $AmRu_2$	**2** $AmRh_2$ $AmRh_3$	**1** $AmPd_3$					**3 to 4** AmSb $AmSb_2$ Am_4Sb_3	**4** AmTe $AmTe_2$ $AmTe_3$ Am_3Te_4	**2** AmI_2 AmI_3
				0	**0**	**0**	**1** $AmOs_2$	**1** $AmIr_2$	**2 to 6** $AmPt_2$ $AmPt_5$		**≥1**			**1 to 5** AmBi		

Fig. 10. Summary of the available data on the Am binary compounds. For each partner element the number of compounds (estimated, calculated or experimentally detected) is reported together with a list of the known stoichiometries. Notice, in several cases, the uncertainty about the number of compounds formed.

enthalpy of formation predicted for compounds at equiatomic composition: to −75 kJ/mol at., for instance, should correspond a number of about five compounds; this number is expected to decrease for lower values of $\Delta_f H$.

The very good agreement with the experimental information may be observed. In the case of U, for example, the weakly negative $\Delta_f H$ values for the elements of the fourth group correspond to the presence of a few compounds stable only at low temperature. Also for Ag the Miedema formula successfully predicts a weakly positive $\Delta_f H$: in fact no Ag–U compound is known even though Ag is surrounded, in the Periodic Table, by compound forming elements.

3. Evaluation of the Miedema parameters for Am

As explained in the preceding paragraph the application of the Miedema formula to the heavy actinides could be very useful not only for confirmation of the previously

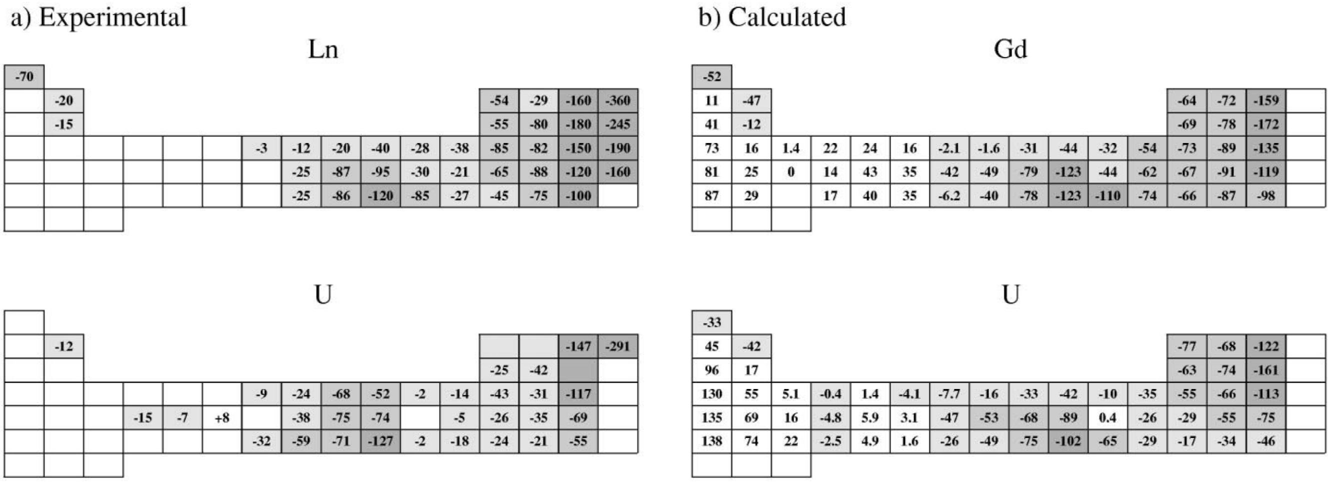

a) Experimental

Ln

-70															
	-20											-54	-29	-160	-360
	-15											-55	-80	-180	-245
						-3	-12	-20	-40	-28	-38	-85	-82	-150	-190
							-25	-87	-95	-30	-21	-65	-88	-120	-160
							-25	-86	-120	-85	-27	-45	-75	-100	

U

	-12													-147	-291
												-25	-42		
						-9	-24	-68	-52	-2	-14	-43	-31	-117	
			-15	-7	+8		-38	-75	-74		-5	-26	-35	-69	
						-32	-59	-71	-127	-2	-18	-24	-21	-55	

b) Calculated

Gd

-52															
11	-47											-64	-72	-159	
41	-12											-69	-78	-172	
73	16	1.4	22	24	16	-2.1	-1.6	-31	-44	-32	-54	-73	-89	-135	
81	25	0	14	43	35	-42	-49	-79	-123	-44	-62	-67	-91	-119	
87	29		17	40	35	-6.2	-40	-78	-123	-110	-74	-66	-87	-98	

U

-33															
45	-42											-77	-68	-122	
96	17											-63	-74	-161	
130	55	5.1	-0.4	1.4	-4.1	-7.7	-16	-33	-42	-10	-35	-55	-66	-113	
135	69	16	-4.8	5.9	3.1	-47	-53	-68	-89	0.4	-26	-29	-55	-75	
138	74	22	-2.5	4.9	1.6	-26	-49	-75	-102	-65	-29	-17	-34	-46	

Fig. 11. Comparison between (a) experimental and (b) calculated (by the Miedema formula) enthalpies of formation. Experimental values here reported are the minimum values known in each system (generally corresponding to different stoichiometries in different systems); the Miedema values, however, are in any case calculated for the equiatomic composition. For the Ln–X systems, experimental values are averaged among the data relevant to different lanthanides; calculated values, however, are referred to Gd. As representative of the An–X systems for both experimental and calculated values U–X systems were selected.

assumed general pattern of compound formation capability, but also for obtaining a few more details about the specific systems (high/low number of compounds, high/low stability, high/low melting points, etc.).

A complete description of the Miedema model has been presented by de Boer et al. [2] and it is briefly illustrated in Appendix A.

In the same book the suggested values of the different elemental semi-empirical parameters appearing in the formula are listed for most elements up to Bi and for Th, U, and Pu. These have been evaluated on the basis of fundamental elemental properties and adjusted by an iterative procedure in order to obtain the best fit of the available thermodynamic or phase equilibrium data.

In a recent paper Gibson et al. [9] made an evaluation of the Miedema parameters for Np and Am, mainly as a function of the fundamental properties of the elements, due to the small experimental knowledge basis presently available for the Np and Am binary systems. For Am they suggested:

$$V^{2/3}(\mathrm{Am}) = 6.77, \quad \Phi^*(\mathrm{Am}) = 3.80$$

$$\text{and} \quad n_{\mathrm{ws}}^{1/3}(\mathrm{Am}) = 1.17$$

On the basis of the empirical relationships previously exposed and mainly summarised in Fig. 8, we have tried to re-determine the Am parameters, as described in the following and systematically considering the Am alloying behaviour with the different elements.

The $V^{2/3}$ parameter is obtained from the atomic volume. From $V(\mathrm{Am}) = 17.63$ cm^3/mol it follows:

$$V^{2/3}(\mathrm{Am}) = 6.77$$

In full agreement with [9].

The Φ^* parameter is correlated to the electronegativity of the element. On this basis, taking in account, on one hand, the Φ^* values assigned to the Ln and An up to Pu and, on the other hand, the electronegativity values (either Pauling or Allred-Rochow) attributed to these elements (transplutonium included) it has been first evaluated in $\Phi^*(\mathrm{Am}) = 3.20$–$3.40$.

The $n_{\mathrm{ws}}^{1/3}$ parameters, in a first approximation, were evaluated in Ref. [2] from the relation $n_{\mathrm{ws}}^2 = K/V$ (K = bulk modulus in GPa, V = atomic volume in cm^3/mol) and then slightly adjusted to get the best agreement between computed and experimental $\Delta_f H$. The relationship finally assumed by [2] between $(K/V)^{1/6}$ and $n_{\mathrm{ws}}^{1/3}$ is represented, for some typical Ln and An, in Fig. 12. This graph has been used to interpolate an initial estimate for Am obtaining $n_{\mathrm{ws}}^{1/3}(\mathrm{Am}) = 1.23$–$1.37$.

By comparing the computed $\Delta_f H$ with the few available experimental $\Delta_f H$ and compound formation data the following final values have been selected:

$$\Phi^*(\mathrm{Am}) = 3.30$$

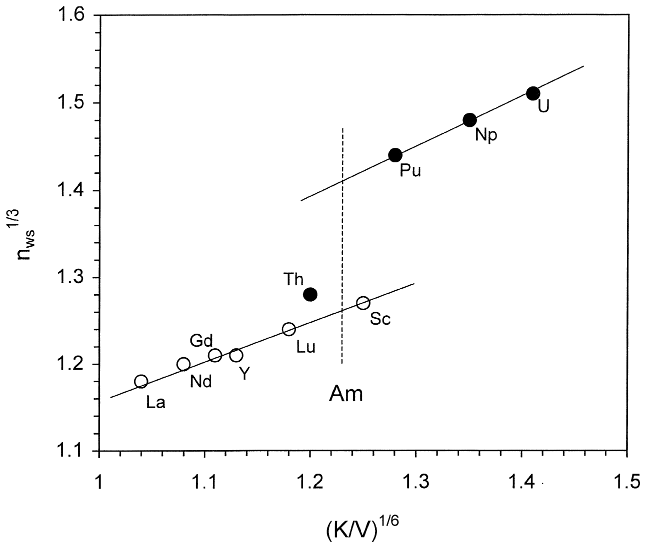

Fig. 12. Miedema $n_{\mathrm{ws}}^{1/3}$ parameter (in density units) plotted against $(K/V)^{1/6}$, where K = bulk modulus (in GPa) and V = atomic volume (in cm^3/mol), for selected Ln (○) and An (●) elements. The vertical dashed line indicates the $(K/V)^{1/6}$ value calculated for Am.

$$n_{\mathrm{ws}}^{1/3}(\mathrm{Am}) = 1.25$$

As for the other parameters, we assumed:

$$a(\mathrm{Am}) = 0.07$$

as de Boer et al. [2] did for the ‘noble’ and trivalent metals, and:

$$R^*(\mathrm{Am}) = 0.7$$

already adopted in Ref. [2] for the rare earths and thorium.

By using the mentioned values the enthalpy of formation of the different Am–X alloys has been computed. The values obtained for the equiatomic compositions are presented in Fig. 13. These data are of course approximate and their reliability is reduced by the uncertainty in the values of the parameters; nevertheless they may give a contribution to the formation of a reasonable picture of the general alloying behaviour of Am complementary to that given in Fig. 10 and in good agreement with it. We may also notice the similarity with the Ln alloying behaviour.

4. Contribution to the Am–X systematics

General and background references to be considered for a systematic description of the chemical and physical properties of Am and its compounds are the following:

- Special issues of the *Atomic Energy Review* [11] for compilations of physico-chemical properties of compounds and alloys of elements important in reactor technology (Th and Pu among the actinides);
- *Handbook on the Physics and Chemistry of Actinides*

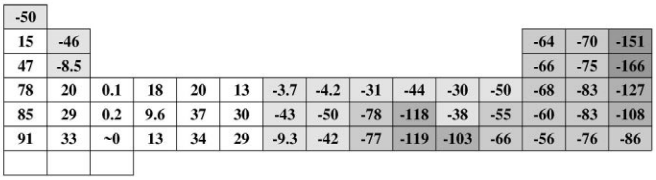

-50														
15	-46											-64	-70	-151
47	-8.5											-66	-75	-166
78	20	0.1	18	20	13	-3.7	-4.2	-31	-44	-30	-50	-68	-83	-127
85	29	0.2	9.6	37	30	-43	-50	-78	-118	-38	-55	-60	-83	-108
91	33	~0	13	34	29	-9.3	-42	-77	-119	-103	-66	-56	-76	-86

Fig. 13. Enthalpy of formation of the Am–X solid alloys at equiatomic composition calculated according to the Miedema model with the parameters evaluated in this work. The data are reported for the different elements arranged according to their position in the Periodic Table (from group 1 to group 15).

[12] for a systematic description and discussion of several physical and chemical properties of the actinides;

- *Handbook on the Physics and Chemistry of Rare Earths* [13] for a comparative parallel description and discussion of several physical and chemical properties of lanthanides and actinides;
- *The Chemical Thermodynamics of Actinide Elements and Compounds* [14] for a series of compilations each concerning the thermochemical properties of a given type of compound for the entire actinide series;
- *Chemical Thermodynamics of Americium* [15] for a systematic description of thermochemical properties of Am and its compounds and complexes.

In the following a systematic description of the Am reactivity with the different elements according to their order in the Periodic Table (compound formation and stability, stoichiometries, structures, etc.) will be presented, tentatively completing the experimental data with those obtained on the basis of the mentioned reference patterns.

4.1. Am–H

Relevant literature references on this system are [16–22].

Olson and Mulford [18] determined the crystal structure of $AmH_{2\pm x}$ (H stoichiometry range from slightly less than 2 to at least 2.7), cF12-CaF_2 type, and AmH_3, hP8-$AsNa_3$ type, and measured the enthalpy of formation of the former.

Roddy [19] used the long-lived ^{243}Am isotope and obtained pressure–temperature–composition data and X-ray measurements. He identified three homogeneous phases: americium solid solution, di-hydride and tri-hydride, investigating the system between pure Am and AmH_3 in the 125–880°C temperature range, at pressures from 10^{-4} to 700 Torr. He also measured enthalpy and entropy of formation of AmH_2.

Gibson and Haire [21] measured the hydrogen pressure and dissociation enthalpy of the hydrides by Knudsen effusion mass spectrometry.

The enthalpy of formation of AmH_2 was measured by Roddy [19] as -190.4 kJ/mol (in comparison with -169 kJ/mol previously determined by Olson and Mulford [18]). More recently the value -177 kJ/mol (-59 kJ/mol of atoms) was obtained by Gibson and Haire [21]. These values may be compared with that computed according to Miedema (see Fig. 13).

In a more recent work Ward and Haschke [22] presented a comprehensive and comparative review on the Ln and An hydride properties, summarising constitutional data and different properties of this system.

For AmH_2 $\Delta_f G = -135$ kJ/mol has been derived in Ref. [15] by using the data given in Ref. [21].

The estimated solubility of H in Am, at different *P* and *T*, and a critical discussion of the previous literature on Am–H are presented by Ward [20] within a systematic review of the An–H systems. A more recent review on the An–H systems was published by Bartscher [23].

4.2. Am-group 1 elements

No compound formation and complete immiscibility both in the solid and liquid phases is expected. We may notice that pure metallic Am may be obtained by reduction with Li of AmF_3 [24].

4.3. Am-group 2 elements

4.3.1. Am–Be

$AmBe_{13}$ (cF112-$NaZn_{13}$) [25] should be the only intermediate compound in the system. Phase equilibria are not known, but, by analogy with Be–Y, Be–Th and Be–U, $AmBe_{13}$ is expected to melt congruently at quite high temperature (about 1800–2000°C) and to form two eutectic equilibria with the pure elements. Am–Be alloys may be prepared by reduction of AmF_3 with Be at *T* higher than 900°C. $AmBe_{13}$ has also been prepared at about 1500°C according to the reaction:

$$AmO_2 + 15Be \rightarrow 2BeO + AmBe_{13}$$

This reaction belongs to the system Am–Be–O, which may be of interest in the field of nuclear engines (compatibility of solid Am with BeO, etc.). According to the literature information available and to our estimate of $\Delta_f G(AmBe_{13})$ (Table 1), an approximate Am–Be–O isothermal section at about 1300 K has been calculated (Fig. 14), by applying the crude approximation of stoichio-

Table 1

Phase	$\Delta_f G$ at 1300 K (kJ/mol at.)	Refs.
Am_2O_3	−276	[26]
AmO_2	−233	[26]
$AmBe_{13}$	−50	Here estimated
BeO	−240	[27]

metric oxides. It is known, however, that both Am_2O_3 and AmO_2 are not stoichiometric and it may be foreseen that both dissolve appreciable amounts of BeO. According to the behaviour of the known Ln oxides, however, the formation of the $(Am,Be)_2O_3$ and $(Am,Be)O_2$ solid solutions or possible ternary phases is not expected to significantly influence the proposed section in the metal-rich region. According to the present calculation, in particular, Am and BeO at about 1300 K should not coexist at equilibrium, but should form Am_2O_3 and $AmBe_{13}$. This conclusion, however, is quite uncertain and, depending also on the temperature, could be reverted if $\Delta_f G$ of any of the binary oxides would change by about 10–20 kJ/mol at.

For comparison we may consider the different behaviour observed in the Pu–Be–O mixtures. The reduction of PuO_2 with metallic Be has been described [28]. At 1000 K BeO is more stable than PuO_2 which is reduced according to the reaction:

$$PuO_2 + 2Be \rightarrow Pu + 2BeO$$

With Be in excess the following reaction is observed:

$$PuO_2 + xBe \rightarrow PuBe_{13} + (x - 15)Be + 2BeO$$

4.3.2. Am–Mg

According to the general pattern of compound formation and the computed $\Delta_f H$, it may be foreseen that the phase diagram contains two or three $AmMg_x$ ($x \geq 1$) compounds. These should decompose or melt at temperatures approximately in the range between the melting temperatures of the pure components.

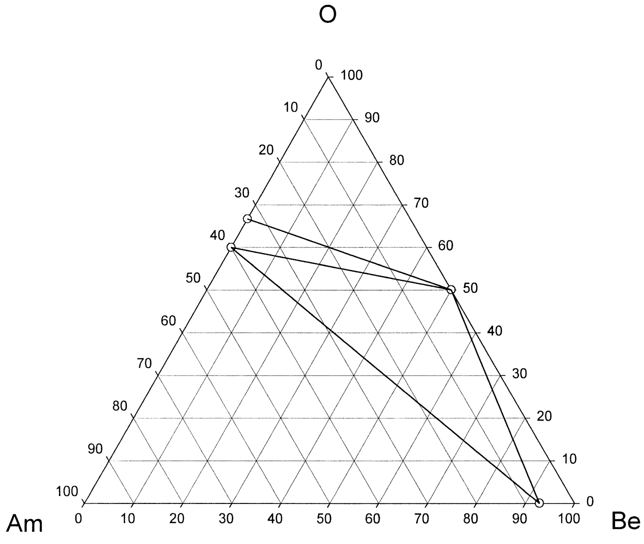

Fig. 14. Estimated schematic Am–Be–O isothermal section at about 1300 K (see text for further comments).

4.3.3. Am–Ca, Sr, Ba

No compound formation, immiscibility in the solid state and wide miscibility gaps in the liquid are expected. Metallic Am may be prepared by reduction of AmF_3 with Ba.

4.4. Am-group 3 elements, lanthanides and actinides

No compound formation from the liquid is expected. A few Am–An systems have been investigated either experimentally (Am–Pu [29], [30], Am–Np [31]) or on the basis of the Brewer valence bond model (Am–U, Np, Pu [32]). Depending on the element crystal structures and atomic radii a variety of situations has been found: complete solid solution ranges (see, for instance, the fcc phase in Am–Pu at high temperature) or wide miscibility gaps both in the solid and liquid state (see, for instance, Am–U) or wide two-phase fields between terminal solid solutions (see, for instance, Am–Np). Ternary Am–Pu–U and Am–Np–Pu phase diagrams were also calculated in Ref. [32].

The reduction of AmF_3 with La at 1200°C is one of the methods for the preparation of elemental Am. The large difference in the volatility of Am and La enable such preparation by distillation to be made [33].

The general inter-Ln alloying behaviour, which perhaps could be useful as a model for the Am–Ln systems, has been described and discussed by Gschneidner and Calderwood [1].

4.5. Am-group 4 elements

No literature information on these systems was found. No compound formation and general alloying behaviour half-way between those of the Am-group 3 and Am-group 5 systems are expected.

4.6. Am-group 5 and group 6 elements

The general scheme of the Am alloying behaviour and a few speculative phase diagrams suggest no compound formation, nearly complete immiscibility in the solid state and very small solubility in the liquid, especially in the case of the heavier and high temperature melting elements like Ta, Mo, W [34] (for Ta see also Ref. [9]). For the lower temperature melting elements of the first transition period, simple eutectic phase diagrams may be expected, as suggested by [35] for Am–Cr.

4.7. Am-group 7 elements

With this group we approach the boundary between compound non forming and compound forming systems. About Mn no information has been found in literature. Probably no compound is formed and a simple eutectic system may be foreseen. For Tc and Re, according to [34], simple systems have been estimated with a very small solubility both in the solid and in the liquid phases. By analogy with systems such as those of Mn with the light Ln, the formation of intermediate phases, possibly metastable or stable only in small temperature ranges, cannot be excluded.

4.8. Am-group 8 elements

Negative enthalpies of formation have been here calculated, especially for Ru and Os (according to Ref. [9], however, for the $AmFe_2$ composition a positive $\Delta_f H$ is calculated). The formation of at least one compound, Laves type, has been described: $AmFe_2$, probably $MgCu_2$ type, $AmRu_2$ and $AmOs_2$, $MgZn_2$ type. $AmOs_2$ may be prepared by arc melting from the elements.

4.9. Am-group 9 elements

Definitely negative enthalpies of formation have been estimated. Several compounds have been experimentally observed: $AmCo_2$ (probably $MgCu_2$ type), $AmRh_2$, $AmIr_2$ ($MgCu_2$ type), $AmRh_3$ ($AuCu_3$ type). Several compounds are probably formed in each system and fairly high melting temperatures may be expected. Peterson and Starzynski [36] obtained the enthalpy of formation of $AmIr_2$ at 1920 K from vapour pressure measurements (Knudsen effusion method): $\Delta_f H(AmIr_2) = -85.4$ kJ/mol at. (the same result was erroneously reported by [37] as -495 kJ/mol).

The highly negative enthalpies of formation of these compounds may be related to the preparation of $AmRh_2$, $AmRh_3$ and $AmIr_2$ by coupled reduction of Am_2O_3 (AmO_2) with Rh (Ir) powder and high purity H_2.

4.10. Am-group 10 elements

$AmNi_2$ (Cu_2Mg type) has been synthesised by arc melting of the two metals. $AmPd_3$ ($AuCu_3$ type) has been obtained by coupled reduction of Am_2O_3 (AmO_2) with fine Pd powder and high purity H_2.

Negative enthalpies of formation have been estimated (less than -100 kJ/mol at. for Pd and Pt). This behaviour may be compared with a few experimental values summarised in Table 2.

By correlation with Nd–Pt and Sm–Pt systems, Peterson and Starzynski [36] estimated the Am–Pt phase diagram suggesting the existence of Am_7Pt_3 (peritectic melting), Am_3Pt_2 (peritectic melting), AmPt (congruent melting), Am_3Pt_4 (peritectic melting), $AmPt_2$ (congruent melting at about 2000°C, the highest in the system, and appreciable solid solubility) and $AmPt_5$ (peritectic melting). Only $AmPt_2$ (Cu_2Mg type [41]) and $AmPt_5$ ($CaCu_5$ type [42]), which form a eutectic with Pt [42], have been experimentally observed.

The coupled reduction of Am_2O_3 (AmO_2) with fine Pt powder and high purity H_2 results in $AmPt_2$ and $AmPt_5$. At low pressure and temperature higher than 1300°C the Pt alloys decompose in Pt and gaseous Am.

4.11. Am-group 11 elements

No data have been reported in literature for the Am–Cu, Ag, Au alloys. The calculated $\Delta_f H$ show a strong variation on passing from Ag to Au (a similar behaviour has been experimentally observed for various Ln and An). For the Am–Au system the formation of several compounds, possibly Au-rich, with high melting points may be foreseen. With Cu and Ag, on the other hand, the formation of compounds cannot be excluded, especially in the Cu(Ag)-rich region, but with low melting points.

4.12. Am-group 12 elements

No data have been reported for Zn. Activity coefficients in Cd of U, Np, Pu and Am have been measured by Roy et al. [43]. Scarce experimental information about Am–Hg is available [44]. Strong interaction between Am and Hg was found and the formation of several solid compounds may be expected in these systems. By analogy with the different Ln and An systems, for the $AmMe_x$ compounds of this group, large values of the stoichiometric ratio (up to $x \cong 11$) may be foreseen. Dilute amalgams may be prepared through electrolysis of Am solutions [45].

Table 2

Phase	Measured quantity	Method and remarks	Refs.
$AmPd_3$	$\Delta_f G$ (J/mol) $= -415\,600 + 37T$	at 1173–1423 K emf, coupled reduction	[38] quoted in [37]
$AmPd_4$	$\Delta_f H$ (kJ/mol at.) $= -83.1$	at 1173–1423 K emf, coupled reduction	[38] quoted in [39]
$AmPt_2$	$\Delta_f G$ (J/mol) $= -413\,000 + 58T$	at 1073–1673 K emf, coupled reduction	[40]
$AmPt_5$	$\Delta_f G$ (J/mol) $= -439\,000 + 48T$	at 1473–1673 K emf, coupled reduction	[40]

4.13. Am-group 13 elements

4.13.1. Am–B

The AmB_4 (tP20-UB_4 type) and AmB_6 (cP7-CaB_6 type) compounds have been identified [46]. A phase diagram has been proposed by analogy with Th–B [16]. The congruent melting of AmB_6 at $T > 2500$°C and the peritectic formation of AmB_4 have also been suggested. AmB_4 was found to lose Am to form AmB_6 during free evaporation in a Knudsen cell [47].

4.13.2. Am–Al

The two intermediate phases $AmAl_2$ (Cu_2Mg type) and $AmAl_4$ (orthorhombic) have been observed [48]. On the basis of the general similarities with the An and Ln alloying behaviour, the formation of other compounds (such as Am_3Al, Am_2Al, AmAl, $AmAl_3$) may be predicted. On the same basis, the maximum melting point in the system (about 1400–1500°C) should correspond to $AmAl_2$.

Al-rich Am–Al alloys have been prepared by reduction of AmO_2 with Al in large excess at 1000–1200°C under a flux of Na_3AlF_6 [24].

4.13.3. Am–Ga, In, Tl

No information is available. The existence of several intermediate phases may be foreseen.

4.14. Am-group 14 elements

4.14.1. Am–C

In literature, data have been reported concerning Am_2C_3, cI40-Pu_2C_3 type [49], and AmC, suggested as cF8-NaCl type [50], of which, however, neither composition nor the oxygen and nitrogen content have been established.

As for the phase equilibria we may refer to the Ln–C [51] and An–C [50] systems. Roughly speaking, two types of Ln–C diagrams may be identified: those formed by the light and the heavy Ln, respectively: the La–C and Y–C phase diagrams may be considered as an example of the two types.

As for the An–C diagrams, it has been observed [50] that with light An (Th to Np) relatively stable monocarbides and, by comparison, rather less stable higher carbides are formed. Starting with Pu increasing stability of the higher carbides is expected, which means growing similarity to the behaviour of the light Ln. This can be explained with an increasing localisation of the f-electrons. Analogies of the Am–C with, for instance, the La–C phase diagram may thus be considered, with the Am_2C_3 phase stable up to high temperature. No indication, however, of a dicarbide has been found. The reactivity of Am_2C_3 with H_2 has been discussed by De Maria [26], by analogy with Pu_2C_3, for which, at $T < 900$ K and low pressure, the formation of the hydride and CH_4 is favoured.

From the systematics of the actinide carbides Holley et al. [52] estimated the thermodynamic properties of Am_2C_3 at 298 K: $\Delta_f H = -151$ kJ/mol, $\Delta_f G = -156$ kJ/mol. These values are very similar to those experimentally determined for the Ln carbides. As for the computed values, however, notice that the Miedema model overestimates the enthalpy of formation of both Ln and An carbides (see Fig. 11).

Ohmichi et al. [53], quoted in Ref. [54], discussed the behaviour of (U,Pu)C containing Am. The loss of this element during the fabrication of the carbide by carbothermic reduction was reported.

4.14.2. Am–C–H

A complex behaviour in the Am–C–H system may be foreseen if an analogy with the Ln–C–H systems is valid. See, for instance, Ref. [51], where data concerning ternary Ln–C–H (Ln = Y, La, Yb) compounds have been reported.

4.14.3. Am–C–Me

The interactions in these ternary systems may be very complex, but, on the other hand, very interesting in view of the properties, possible applications, etc. of these materials. Very scant data being available in literature, the description (with isothermal sections, crystal structure tables, etc.) of ternary Ln–C–Me and An–C–Me systems with several Me elements reported by Refs. [51] and [50], respectively, may constitute a general references framework. In the same reviews data concerning simple and complex nitrides are also included.

4.14.4. Am–Si

Several compounds have been identified and their structures determined [55,56]. These are: Am_5Si_3 (tI32-W_5Si_3 type), AmSi (oP8-FeB type), Am_3Si_5 (possibly a solid solution range up to Am_2Si_3 exhibiting a defective hP3-AlB_2 type structure), $AmSi_2$ (tI12-$ThSi_2$). These were generally prepared at 900–1100°C by the reaction:

$$4AmF_3 + (3 + 4x)Si \rightarrow 4AmSi_x + 3SiF_4$$

According to Ref. [56] all compounds should melt (congruently or incongruently) between 900 and 1000°C. Notice, however, that much higher melting temperatures would be foreseen by analogy with Ln–Si and An–Si systems.

AmSi possibly undergoes a phase transformation between 540 and 670°C.

4.14.5. Am–Ge, Sn, Pb

No information has been found in literature. The computed enthalpies of formation and the analogies with the similar Ln and An systems suggest the formation of a number of intermediate phases. For instance $AmSn_3$ and $AmPb_3$ showing an $AuCu_3$ type structure could be predicted.

4.15. Am-group 15 elements

4.15.1. Am–N

No phase diagram is available. The existence of AmN (cF8-NaCl type) was first reported by Akimoto [57] and then prepared also in Refs. [58,59]. Even in the presence of ammonia/hydrogen mixtures, which corresponds to quite high effective nitrogen pressure, no higher nitrides were found, corresponding to those in the earlier An–N systems. Vaporisation behaviour of (Pu,Am)N has been studied by Knudsen cell mass spectrometric analysis [54]. The second law enthalpy of formation from N_2 and liquid Am at 1600 K was estimated to be −147 kJ/mol at.

4.15.2. Am–P, As, Sb, Bi

No phase diagram is available. Several compounds have been observed and their crystal structures described. Monopinictides AmP, AmAs, AmSb and AmBi belong to the cF8-NaCl type. The possible formation of Am_4X_3, Am_3X_4 and AmX_2 compounds has been suggested or described [60]. For Sb, the crystal structures of $AmSb_2$ (oC24-$SmSb_2$ type [61]) and Am_3Sb_4 (cI28, anti-Th_3P_4 type [58]) have been determined.

On the basis of the computed enthalpies of formation and by analogy with Ln–X and An–X systems, phase diagrams showing very high melting points for compositions close to the equiatomic ratio may be predicted.

Am–Sb and Am–Bi alloys have been prepared by reaction between the two elements (for instance, Sb vapour over Am metal or Am hydride).

The ternary AmSbTe phase (tP6, anti-Cu_2Sb type) was also prepared in Ref. [61].

4.16. Am-group 16 elements

4.16.1. Am–O

A few compounds have been described: Am_2O_3, AmO_2 and, possibly, AmO.

The highest binary oxide of Am is the AmO_2 (more precisely AmO_{2-x} with $0 \leq x \leq 0.35$) which is formed while calcinating salts of Am in air or oxygen up to 900°C. The melting temperature was estimated, by extrapolation of the melting points of other An dioxides, to be about 2170°C. Notice however that above 900°C the Am dioxide starts to lose oxygen. The dioxide crystallises in the cF12-CaF_2 structure. AmO_2 may be dissolved in molten KOH–NaOH in the presence of O_2. Morss and Fuger [62] measured the enthalpy of dissolution of AmO_2 in a K_2SO_4–KI solution and from their results [15] calculated $\Delta_f H(AmO_2, 298\text{ K}) = -932$ kJ/mol and $\Delta_f G(AmO_2, 298\text{ K}) = -875$ kJ/mol.

Two crystal forms of Am_2O_3 have been reported: the cubic cI80-Mn_2O_3 low-temperature structure and the hexagonal hP5-La_2O_3 high-temperature form. The transformation should occur between 700 and 900°C. A third, probably metastable, monoclinic structure was also reported [63]. The hexagonal sesquioxide was found to melt at about 2200°C [64]. It may be obtained from the dioxide by reduction (with H_2 or $H_2 + N_2$). Thermodynamic properties have been studied in Ref. [65] by dissolving hexagonal Am_2O_3 in hydrochloric acid in a microcalorimeter obtaining $\Delta_f H(Am_2O_3, 298\text{ K}) = -1690$ kJ/mol. From this, Silva et al. [15] calculated $\Delta_f G(Am_2O_3, 298\text{ K}) = -1613$ kJ/mol.

Two different Am–O phase diagrams (limited to the $0.59 \leq x(O) \leq 0.67$ composition range) have been tentatively proposed in Refs. [15,66]: they are reported in Fig. 15.

More recently, Zhang et al. [67] estimated thermodynamic data for the Am oxides to calculate the Am–Mg–O phase equilibria.

The existence of AmO (cF8-NaCl type) has been reported by Schultz [68] but only on the microgram scale. This work led to reporting a lattice parameter for the compound, yet the existence of AmO is still questionable. According to Ref. [15], AmN has a similar NaCl type structure and it seems likely that this was an Am(O,N) solid solution, similar to the so-called plutonium monoxide which is now known to be a Pu(C,O,N) phase.

A discussion of the estimated thermodynamic properties has been carried out by De Maria [26] who confirmed that,

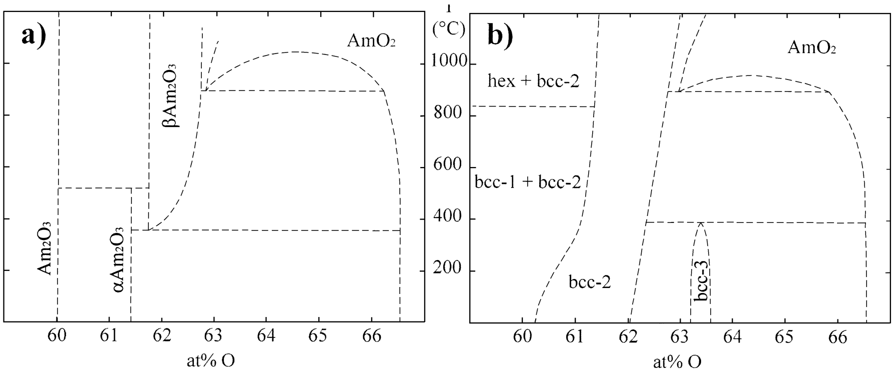

Fig. 15. Am–O phase diagrams in the composition range $0.59 \leq x(O) \leq 0.67$ tentatively proposed in (a) Ref. [66] and (b) Ref. [15].

among several conjectured Am oxide reactions with H_2 in the temperature range 400–1400 K, the reduction of AmO_2 to Am_2O_3 is the only feasible one.

Ternary oxides of transuranium elements with transition elements have been described and discussed by Tabuteau and Pagès [69]. Properties of a number of crystal structure types and a few phase diagrams have been presented. For Am, for instance, information is reported about simple and complex titanates, vanadates, niobates, tantalates, tungstates, perrhenates. A list and a description of ternary and quaternary Am oxides is reported in Ref. [15].

As for the reactions of Am with oxygen containing compounds such as CO, CO_2, H_2O, etc. some indication could possibly be obtained by analogy with the rare earths. See, for instance, the description of typical reactions of thin films of Ln reported in Ref. [70].

Aqueous oxide and hydroxide complexes have been the subject of several investigations (see Ref. [15] for a summary). As an example, Fig. 16 gives the calculated distribution diagram of americium species at room temperature in standard aqueous solutions in the pH 6–12 range [15].

4.16.2. Am–S, Se, Te

The Ln–X and An–X phase diagrams are not very well defined and several of them would require a more or less complete revision. Generally these systems show the existence of the Ln–X or An–X 1:1 NaCl type compounds, congruent melting with very high melting points (up to 2000–2500°C for the sulphides and lower for Se and Te) and of a number of LnX_x and AnX_x compounds with stoichiometric ratios $x>1$.

In the specific case of Am the following compounds have been identified: AmS_2 and $AmTe_2$ (structures related to the tP6-Cu_2Sb type), AmS, AmSe and AmTe (cF8-NaCl type), Am_2S_3 (tentatively related to the α-Ce_2S_3 orthorhombic structure), Am_3S_4 (also denoted as γ-Am_2S_3), Am_3Se_4 and Am_3Te_4 (cI28-Th_3P_4 type).

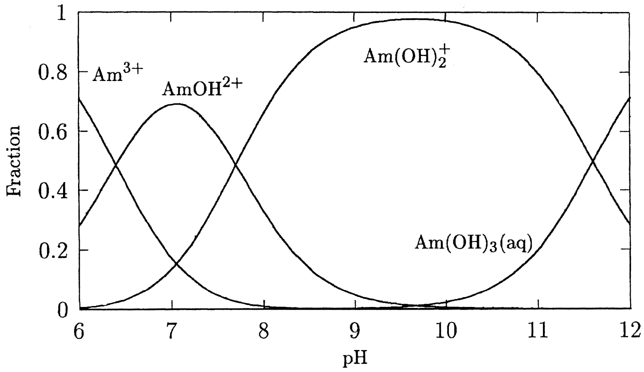

Fig. 16. Calculated distribution diagram for americium species at 25°C in standard aqueous solutions ($I=0$) in the range $6\leq pH\leq 12$, according to Ref. [15].

4.17. Am-group 17 elements

The americium halides are not specially relevant in the framework of this review. Their formulae and characteristics are reported in Ref. [15].

The following compounds have been described: $AmCl_2$ (orthorhombic, $PbCl_2$ type), $AmBr_2$ (tetragonal, $EuBr_2$ type), AmI_2 (monoclinic, EuI_2 type), AmF_3 (hexagonal, LaF_3 type), $AmCl_3$ (UCl_3 type), $AmBr_3$ and AmI_3 (orthorhombic, $PuBr_3$ type), AmF_4 (monoclinic, UF_4 type), AmF_6 (formed under highly fluorinating conditions). Crystal structure data and general properties of Ln and An halides have been described by Eick [71].

For Am fluorides an evaluation of thermodynamic properties has been carried out in Refs. [15,72]. Selected values concerning the Am three-halides and tetra-fluoride are here reported as an example:

$$\Delta_f H(AmF_3, 298\ K) = -1588\ kJ/mol,$$
$$\Delta_f S(AmF_3, 298\ K) = 128\ J/mol\ K$$

$$\Delta_f H(AmCl_3, 298\ K) = -978\ kJ/mol,$$
$$\Delta_f S(AmCl_3, 298\ K) = 165\ J/mol\ K$$

$$\Delta_f H(AmBr_3, 298\ K) = -810\ kJ/mol,$$
$$\Delta_f S(AmBr_3, 298\ K) = 205\ J/mol\ K$$

$$\Delta_f H(AmI_3, 298\ K) = -612\ kJ/mol,$$
$$\Delta_f S(AmI_3, 298\ K) = 234\ J/mol\ K$$

$$\Delta_f H(AmF_4, 298\ K) = -1720\ kJ/mol,$$
$$\Delta_f S(AmF_4, 298\ K) = 149\ J/mol\ K$$

Further thermodynamic data concerning halides and oxy-halides are reported in Ref. [15].

Am^{III} precipitates as fluoride (pink) when HF or a solution of F ions is added to an acid solution of Am^{III}.

5. Final remarks

In conclusion we may notice the good agreement between the few and, in several cases approximate, experimental data and the general alloying behaviour depicted for Am.

The schemes reported in Figs. 8–11 may be useful for predicting and interpolating characteristics of specific combinations. It may also help to define a few 'crucial' systems a good experimental investigation of which may improve the general reference framework (giving for instance help for a more accurate definition of the Miedema parameters, etc.). Just as an example, systems such as Am–Mn, Am–Bi, could be considered.

As previously observed the Ln–Mn and An–Mn systems are at the boundary between those characterised by compound-forming and non-forming ability. An experimentally based definition of this point for Am may be useful. An investigation based on the examination of a number of alloys after long annealing procedures should probably be adopted. In the case of the Ln–Mn systems, for instance, no compound is observed for La and Ce (miscibility gaps in the liquid state), a metastable phase $PrMn_2$ is formed in the Pr–Mn system and phases stable only at high temperature are observed for Pr and Nd (Pr_6Mn_{23}, $NdMn_2$, Nd_6Mn_{23}). These compounds are generally retained after cooling at room temperature but slowly decompose (typically in 1 month at 400°C) in the equilibrium mixtures of the component elements. A number of stable compounds are formed in the systems of Mn with the heavier Ln.

For the Am–Bi system (as for Am–Sb, Am–Te, etc.) it should be possible, by using small quantities of the components, and possibly by means of different techniques, to perform reliable thermodynamic measurements (of enthalpy of formation, for instance) and give reference values for a general assessment of Am alloy thermodynamics. To this end another crucial system may be Am–Al.

For selected binary intermetallic Am–Me systems, and for the few known and well characterised compounds, the determination of melting points or other invariant equilibrium temperatures (eutectic, peritectic, etc.) could give other useful information, relatively easy to obtain even with small amounts of alloys. These data could also represent, by comparison with the same data relevant to the corresponding An–Me or Ln–Me systems, an indirect information on the stability of the Am–Me compounds. Stability and equilibrium data, even if incomplete, could be used as input for the calculation of Am–Me phase diagrams.

Acknowledgements

The authors would like to dedicate this article to the memory of Dr. Prince, remembering with gratitude his valuable teaching. R. Ferro would particularly like to remember Dr. Prince with appreciation for his advice, and suggestions frequently given from the early 1980s onwards. With reference to this paper, the authors acknowledge with warm thanks valuable advice received from Professor G. De Maria and co-workers of the Chemistry Department, University of Rome ‘La Sapienza’. Thanks are due also to Dr. Bidoglio of the Environment Institute, Joint Research Centre, Ispra, and Dr. I. Ansara of the LTPCM Laboratory, Institut Nationale Politechnique de Grenoble who very kindly provided us with special references and their own publications. Italian ‘Ministero dell’Università e della Ricerca Scientifica e Tecnologica’ is acknowledged with thanks for the financial support given in the framework of a National Research Project entitled ‘Leghe e composti intermetallici: stabilità termodinamica, proprietà fisiche e reattività’.

Appendix A

The Miedema enthalpies of formation have been calculated by means of the computer program reported in Ref. [2]. The values may be expressed as follows:

$$\Delta_f H = \frac{f(x_A,x_B,V_A^{2/3},V_B^{2/3},a_A,a_B,\Phi_B^* - \Phi_A^*)}{\frac{1}{n_{ws_A}^{1/3}} + \frac{1}{n_{ws_B}^{1/3}}} \cdot P \cdot \left[-(\Phi_B^* - \Phi_A^*)^2 + \frac{Q}{P}\left(\frac{1}{n_{ws_B}^{1/3}} + \frac{1}{n_{ws_A}^{1/3}}\right)^2 - \frac{R}{P} \right] + (x_A H_A^T + x_B H_B^T)$$

where:

- indices A and B represent the two alloying elements;
- Φ^*, $V^{2/3}$, $n_{ws}^{1/3}$, a, R^*, H^T are the semi-empirical parameters evaluated and reported in Ref. [2].
- f function is an expression in principle obtained by a recursive procedure. It depends on the alloy composition (x_A, x_B), the elemental atomic volumes (V_A, V_B), the difference of the chemical potential for electronic charge ($\Phi_A^* - \Phi_B^*$), the a_A and a_B empirical parameters;
- $n_{ws}^{1/3}$, is the electron density at the boundary of the Wigner–Seitz atomic cell;
- P empirical parameter assumes different values according to whether A and B are both transition, both non-transition, or transition and non-transition elements; the square bracket includes two empirical parameters: Q/P is assumed to be constant and R/P, which is zero when A and B are both transition metals, is given by the product of two elemental constants R_A^* and R_B^* when A and B are transition and non-transition elements, respectively.
- In the last additive term H^T parameters are non-zero only for H, B, C, Si, Ge, N, P.

References

[1] K.A. Gschneidner Jr., F.W. Calderwood, in: K.A. Gschneidner Jr., L. Eyring (Eds.), Handbook on the Physics and Chemistry of the Rare Earths, Vol. 8, Elsevier, 1986, pp. 1–161.

[2] F.R. de Boer, R. Boom, W.C.M. Mattens, A.R. Miedema, A.K. Niessen, Cohesion in Metals — Transition Metal Alloys, in: F.R. de Boer, D.G. Pettifor (Eds.), Cohesion and Structure Series, Vol. 1, North Holland, New York, 1988.

[3] P. Villars, K. Mathis, F. Hulliger, in: F.R. de Boer, D.G. Pettifor (Eds.), The Structure of Binary Compounds, Elsevier, Amsterdam, 1989, pp. 1–103.

[4] W.C. Leslie, E. Hornbogen, in: R.W. Cahn, P. Haasen (Eds.), Physical Metallurgy, IV Edition, Elsevier, Amsterdam, 1996.

[5] E.K. Molchanova, in: The Physical Metallurgy of Titanium Alloys, ASM International, Metals Park, OH, 1984, p. 43.

[6] P. Villars, K. Brandenburg, M. Berndt, S. Le Clair, A. Jakson, Y.-H. Pao, B. Igelnik, M. Oxley, B. Bakshi, P. Chen, S. Iwata, in: 13th International Conference on Solid Compounds of Transition Elements, Stresa, Italy, 4–7/4/2000, 2000.

[7] J.L. Smith, E.A. Kmetko, J. Less-Common Met. 90 (1983) 83–88.

[8] U. Benedict, W.B. Holzapfel, in: K.A. Gschneidner Jr., L. Eyring, G.R. Choppin, G.H. Lander (Eds.), Handbook on the Physics and Chemistry of the Rare Earths, Vol. 18, Elsevier, Amsterdam, 1993, pp. 245–300.

[9] J.K. Gibson, R.G. Haire, T. Ogawa, J. Nucl. Mater. 273 (1999) 139–145.

[10] C. Rubbia, Report ASI-WG-04, ASI, Roma, Italy, 1999.

[11] Atomic Energy Review, Special Issues 1–9, IAEA, Vienna, 1966–1983.

[12] A.J. Freeman, C. Keller (Eds.), Handbook on the Physics and Chemistry of Actinides, Vols. 1–6, Elsevier, Amsterdam, 1984–1991.

[13] K.A. Gschneidner Jr., L. Eyring, G.R. Choppin, G.H. Lander (Eds.), Handbook on the Physics and Chemistry of Rare Earths, Vols. 17–19, Elsevier, Amsterdam, 1993–1994.

[14] The Chemical Thermodynamics of Actinide Elements and Compounds, Parts 1–12, IAEA, Vienna, 1976–1992.

[15] R.J. Silva, G. Bidoglio, M.H. Rand, P.B. Robouch, H. Wanner, I. Puigdomenech, in: Chemical Thermodynamics of Americium, Elsevier/North-Holland, Amsterdam, 1995.

[16] T.B. Massalski (Ed.), 2nd Edition, Binary Alloy Phase Diagrams, Vols. 1–3, ASM, Metals Park, OH, 1990.

[17] P. Villars, A. Prince, H. Okamoto, in: Handbook of Ternary Alloy Phase Diagrams, Vols. 1–2, ASM International, Metals Park, OH, 1995.

[18] W.M. Olson, R.N.R. Mulford, J. Phys. Chem. 70 (1966) 2934–2937.

[19] J.W. Roddy, J. Inorg. Nucl. Chem. 35 (1973) 4141–4148.

[20] J.W. Ward, in: A.J. Freeman, C. Keller (Eds.), Handbook on the Physics and Chemistry of the Actinides, Vol. 3, Elsevier, Amsterdam, 1985, pp. 1–74.

[21] J.K. Gibson, R.G. Haire, J. Phys. Chem. 94 (1990) 935–939.

[22] W. Ward, M. Haschke, in: K.A. Gschneidner Jr., L. Eyring, G.R. Choppin, G.H. Lander (Eds.), Handbook on the Physics and Chemistry of the Rare Earths, Vol. 18, Elsevier, Amsterdam, 1994, pp. 293–363.

[23] W. Bartscher, Diffusion and Defect Data Part B (Solid State Phenomena) 49–50 (1996) 159–238.

[24] C. Keller, in: Gmelin Handbuch der Anorganiscen Chemie. Band 39. Transurane. Teil B3, Springer, Berlin, 1977, pp. 267–271.

[25] U. Benedict, K. Buijs, C. Dufour, J.C. Toussaint, J. Less-Common Met. 2 (1975) 345–354.

[26] G. De Maria, report ASI-WG-15, ASI, Roma, Italy, 1999.

[27] M.W. Chase Jr., in: NIST-JANAF Thermochemical Tables, 4th Edition, NIST, Gaithersburg, USA, 1998, Part 1/2.

[28] G. Michaud, R.R. Boucher, Can. J. Phys. 38 (1960) 555.

[29] T.G. Chart, N.J. Pugh, report DMM(A), N.P.L., Teddington, UK, 1990, p. 16 (Met. Abstr., 23-11-0858).

[30] V.D. Shushakov, N.S. Kosulin, N.T. Chebotarev, Ser. Mater. Sci. New Mater. 3 (1990) 14–15.

[31] J.K. Gibson, R.G. Haire, J. Nucl. Mater. 195 (1992) 156–165.

[32] T. Ogawa, J. Alloys Comp. 194 (1993) 1–7.

[33] J. Peterson, in: Gmelin Handbuch der Anorganiscen Chemie. Band 31. Transurane. Teil B1, Springer, Berlin, 1976, pp. 57–67.

[34] H.F. Wu, L. Brewer, J. Phase Equil. 17 (1996) 36–39.

[35] M. Venkatraman, J.P. Neumann, D.E. Peterson, Bull. Alloy Phase Diagrams 6 (1985) 415–416.

[36] D.E. Peterson, J.S. Starzynski, J. Less-Common Met. 105 (1985) 273–281.

[37] H. Kleykamp, J. Nucl. Mater. 201 (1993) 193–217.

[38] S. Möbius, Report KFH2634, Kernforschungzentrum, Karlsruhe, Germany, 1978 (quoted in Ref. [39]).

[39] C. Colinet, A. Pasturel, in: K.A. Gschneidner Jr., L. Eyring, G.R. Choppin, G.H. Lander (Eds.), Handbook on the Physics and Chemistry of the Rare Earths, Vol. 19, Elsevier, Amsterdam, 1994, pp. 479–647.

[40] S. Mobius, L. Hellwig, C. Keller, J. Less Common Met. 121 (1986) 43–48.

[41] D.J. Lam, A.W. Mitchell, J. Nucl. Mater. 44 (1972) 279–284.

[42] V.M. Radchenko, A.G. Seleznev, L.S. Lebedeva, R.R. Droznik, M.A. Ryabinin, V.D. Shushakov, Radiokhimiya 31 (3) (1989) 15–20.

[43] J.J. Roy, L.F. Granthan, D.L. Grimmett, S.P. Fusselman, C.L. Krueger, T.S. Storvick, T. Inoue, Y. Sakamura, N. Takahashi, J. Electrochem. Soc. 143 (1996) 2487–2492.

[44] C. Guminski, J. Phase Equil. 16 (1995) 333.

[45] H. Blank, R. Schenkel, in: Gmelin Handbuch der Anorganiscen Chemie. Band 39. Transurane. Teil B3, Springer, Berlin, 1977, pp. 1–266.

[46] H.A. Eick, R.N.R. Mulford, J. Inorg. Nucl. Chem. 31 (1969) 371–375.

[47] P.E. Potter, in: A.J. Freeman, C. Keller (Eds.), Handbook on the Physics and Chemistry of the Actinides, Vol. 6, Elsevier, Amsterdam, 1991, pp. 39–73.

[48] M.E. Kassner, D.E. Peterson, Bull. Alloy Phase Diagrams 10 (1989) 277.

[49] A.W. Mitchell, D.J. Lam, J. Nucl. Mater. 36 (1970) 110–112.

[50] H. Holleck, in: A.J. Freeman, C. Keller (Eds.), Handbook on the Physics and Chemistry of the Actinides, Vol. 4, Elsevier, Amsterdam, 1986, pp. 209–307.

[51] G.-Y. Adachi, N. Imanaka, F. Zhang, in: K.A. Gschneidner Jr., L. Eyring (Eds.), Handbook on the Physics and Chemistry of the Rare Earths, Vol. 15, Elsevier, Amsterdam, 1991, pp. 1–189.

[52] C.E. Holley Jr., M.H. Rand, E.K. Storms, in: The Chemical Thermodynamics of the Actinide Elements and Compounds, IAEA, Vienna, 1984, Part 6.

[53] T. Ohmichi, Y. Suzuki, Y. Arai, T. Sasayama, A. Maeda, J. Nucl. Mater. 139 (1986) 253.

[54] T. Ogawa, T. Ohmichi, A. Maeda, Y. Arai, Y. Suzuki, J. Alloys Comp. 224 (1995) 55–59.

[55] F. Weigel, F.D. Wittmann, R. Marquart, J. Less Common Met. 56 (1977) 47–53.

[56] F. Weigel, F.D. Wittmann, W. Schuster, R. Marquart, J. Less Common Met. 102 (1984) 227–238.

[57] Y. Akimoto, J. Inorg. Nucl. Chem. 29 (1967) 2650–2652.

[58] J.-P. Charvillat, U. Benedict, D. Damien, W. Müller, Radiochem. Radioanal. Lett. 20 (1975) 371–381.

[59] V.M. Radchenko, M.A. Ryabinin, A.G. Seleznev, E.V. Shimbarev, L.V. Sudakov, I.I. Kapshukov, V.Ya. Vasil'ev, Sov. Radiochem. 24 (1982) 144–146.

[60] J.-P. Charvillat, Crystal chemistry of transuranium pnictides, report CEA-R-4933 CEA, Saclay, France, 1978, p. 364. (Chem. Abs. 92-32335D).

[61] J.-P. Charvillat, D. Damien, A. Wojakowski, Rev. Chim. Miner. 14 (1977) 178–188.

[62] L.R. Morss, J. Fuger, J. Inorg. Nucl. Chem. 43 (1981) 2059–2064.

[63] U. Berndt, R. Tanamar, D. Maier, C. Keller, Inorg. Nucl. Chem. Lett. 10 (1974) 315–321.

[64] T.D. Chikalla, C.E. McNeilly, J.L. Bates, J.J. Rasmussen, Proc. Int. Colloq. High Temperature Phase Transformations, CNRS 205 (1973) 351–360.

[65] L.R. Morss, D.C. Sonnenberger, J. Nucl. Mater. 130 (1985) 266–272.

[66] H. Okamoto, J. Phase Equil. 12 (1991) 696–697.

[67] H. Zhang, R.J.M. Konings, M.E. Huntelaar, E.P.H. Cordfunke, J. Nucl. Mater. 250 (1997) 88–95.

[68] W.W. Schultz, report TID26971, ERDA, Oak Ridge, TN, USA, 1976.

[69] A. Tabuteau, M. Pagès, in: A.J. Freeman, C. Keller (Eds.), Handbook on the Physics and Chemistry of the Actinides, Vol. 3, Elsevier, Amsterdam, 1985, pp. 185–241.

[70] M. Gasgner, in: K.A. Gschneidner Jr., L. Eyring (Eds.), Handbook on the Physics and Chemistry of the Rare Earths, Vol. 20, Elsevier, Amsterdam, 1995, pp. 105–206.

[71] H.A. Eick, in: K.A. Gschneidner Jr., L. Eyring, G.R. Choppin, G.H. Lander (Eds.), Handbook on the Physics and Chemistry of the Rare Earths, Vol. 18, Elsevier, Amsterdam, 1994, pp. 365–411.

[72] P.D. Kleinschmidt, J. Alloys Comp. 213–214 (1994) 169–178.